ITTC Quality System Manual
Recommended Procedures and Guidelines

Visual Description and Measurement of Cavitation Events

Alves Pereira F., Boucheron R., Boucetta D., Fetherstonhaugh C., Krol P., Pang Y., Park C., Sato K., Straka W. A., Viitanen V.

7.5	Process Control
7.5-02	Testing and Extrapolation Methods
7.5-02-03	Propulsion
7.5-02-03-03	Cavitation
7.5-02-03-03.2	Visual Description and Measurement of Cavitation Events

Updated / Edited by	Approved
Specialist Committee on Cavitation and Noise of the 30th ITTC	30th ITTC 2024
Date 05/2024	Date 09/2024
© 2024 ITTC.A Switzerland	DOI:

Table of Contents

Abstract

The purpose of this procedure is to ensure that the visual description of cavitation events observed during model-scale cavitation tests are consistent amongst ITTC member organisations. The procedure considers propellers and podded propulsors and can be extended to other hydrodynamic devices. Measurement methodologies for the quantitative description of cavitation events are reviewed.

Visual Description and Measurement of Cavitation Events

1. PURPOSE OF PROCEDURE

The purpose of this procedure is to ensure that the visual description of cavitation events observed during model-scale cavitation tests are consistent amongst ITTC member organisations. The procedure is designed for propellers and podded propulsors and can be extended to other hydrodynamic devices.

The procedure also introduces measurement methodologies for the quantitative description of cavitation events. References are given for some experimental approaches implemented to this date. However, these do not constitute a standard nor supersede other, similar methods not cited.

2. VISUAL DESCRIPTION OF CAVITATION ON CONVENTIONAL PROPELLERS

2.1 Introduction

It is standard practice in cavitation testing laboratories to include sketches, photographs or high-speed video recordings of cavitation patterns in test reports. Descriptive terms are used to identify the various types of cavitation observed during tests on propellers, typified below in Figure 1.

Description of cavitation events should contain information on cavity location, size, structure, and dynamics, as well as proper references to the prevailing flow dynamics. The number of alternative descriptions for cavity structure should be limited to the most commonly used.

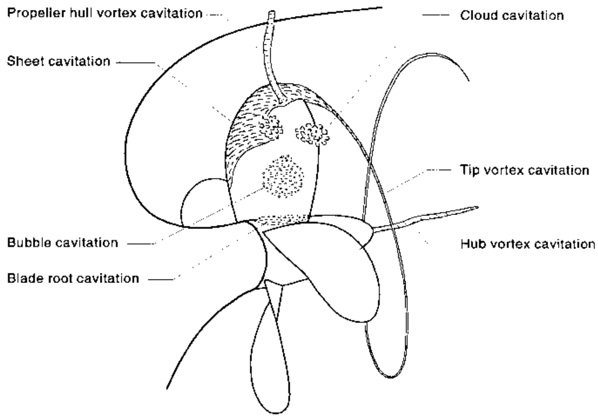

Figure 1: Cavitation types

2.2 Description

The following descriptive types of cavitation are recommended.

- cloud
- sheet
- streak
- bubble - large, small
- root
- vortex - attached, trailing detached, leading edge, propeller-hull, hub
- supercavitation.

Along with the categories mentioned above, information on cavity location, in particular with regard to propellers, should be specified as follows:

- radial location:
  - fraction of tip radius
  - blade tip
  - root fillet
  - tip (duct) gap
  - hub

- chordwise location:
  - fraction of chord
  - leading edge
  - trailing edge
- suction side (back)
- pressure side (face)
- location in wake

Cavity size should be described in terms of body dimensions if developed cavitation exists, for instance by defining the fraction of blade area which is covered by a certain type of cavitation.

Typical examples of cavity types are shown in Figure 2 through Figure 5. Descriptions of some cavity types are below:

sheet cavitation

- initiates along the leading edge and closes on the foil surface along the chord. Usually thin, smooth, transparent, foamy in the closure region. Can become unsteady e.g. at increased flow angle of attack. Can also start around section of maximum thickness.

cloud cavitation

- usually develops from the break-up of unsteady sheet cavitation. Recognizable in the form of cloud-like vapor pockets released in the wake of the sheet cavity.

streak cavitation

- special form of bubble cavitation, narrow and elongated, usually forming at isolated roughness spots and other imperfections on the blade surface or at the leading edge.

bubble cavitation

- large bubble type, usually isolated and travelling along the suction side (back) of foil.
- small bubble-type cavitation indicative of propellers with blade sections having a smooth distribution of the pressure coefficient C_p (i.e. no pronounced suction peak).

vortex cavitation

- leading edge vortex cavitation occurs along the leading edge, usually at high loading conditions.
- attached tip vortex cavitation occurs very near the blade tip, often attached to the blade; can be intermittent at inception, stable when developed.
- trailing, detached tip vortex cavitation incepts downstream of the blade tip; can be stable or bursting.
- propeller-hull, free vortex extending from hull to propeller disk, at low speed, high loading conditions, e.g. at very low advance ratios.

root cavitation

- thick three-dimensional cavitation occurring at the blade root, commonly seen on controllable pitch propellers (CPP).

super cavitation

- initiates like sheet cavitation but extends beyond the trailing edge, with closure in the fluid downstream.

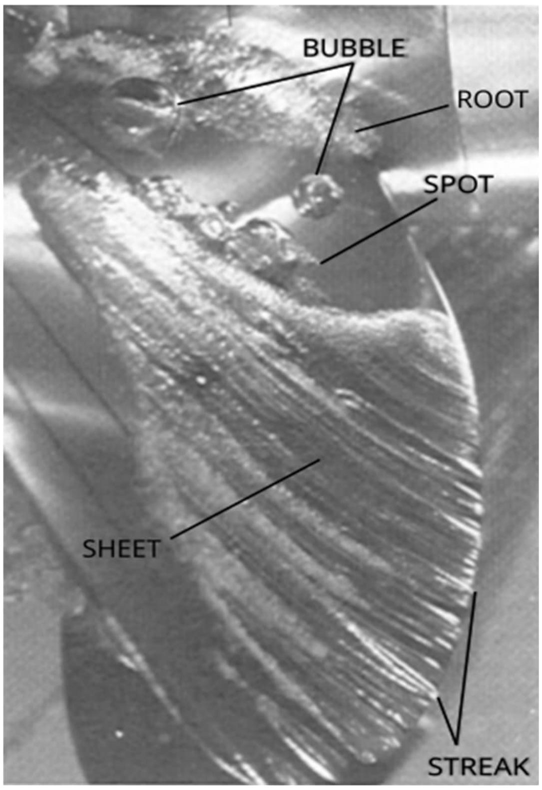

Figure 2: Leading edge, streak, large bubble and root cavitation

Figure 3: Small bubble and streak cavitation

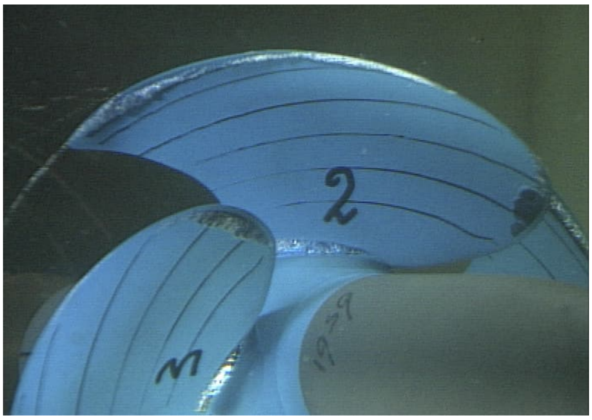

Figure 4: Attached leading edge vortex and tip vortex, leading edge sheet, and root cavitation

Figure 5: Supercavitation

other forms

- hub vortex
- tip gap leakage vortex (ducted propeller)
- CPP blade bolt cavitation
- cavitation in separated flow regions, high blade angle of attack, and wake.

cavity dynamics can be categorized as:

- steady
- periodic
- unsteady
- non-periodic
- transient or travelling
- intermittent
- unstable
- bursting.

When possible, to complete the description requirements stated above, reference should be made to the type of flow associated with certain cavitation phenomena, e.g.

- laminar boundary layer
- turbulent boundary layer
- steady flow
- unsteady flow
- separated flow
- free vortices
- shear layers
- incoming wake flows (uniform, non-uniform or unsteady)
- upstream vortex structures (hull appendages, such as roll fins, keel vortex)
- ventilated flow.

The list of cavitation forms should not be regarded as fully comprehensive, but should be extended, if necessary. The use of more than one term for the same phenomenon should be avoided, and descriptions should be as complete as possible.

2.3 Propeller model marking

Marking is made on certain model components to facilitate the interpretation of cavitation extent and location. Great care must be exercised to use very thin painting or marking pen lines to avoid artificial sites for initiation of sheet, bubble or streak cavitation. For painting, measurement of thickness in different locations can be done with ultrasonic coating thickness gauges or other means. A thickness of less than 0.01 mm is desirable. Marking is recommended as follows:

- Paint or mark blade number on each side of each blade, or/and on the hub near the blade root.
- Paint or mark lines along constant radius lines at selected r/R values, suction side (SS) and pressure side (PS), typically at 0.5, 0.7, and 0.9 radius, but also at regular steps from root to tip (e.g. every 0.1R).
- Paint or mark the mid chord line and/or the reference line, SS and PS.
- Paint or mark spanwise lines at regular steps along the chord (e.g. every 10% of chord on each of the marked radius lines above).
- Marking on the hub and bossing to help determine a blade relative position angle.

2.4 Reporting cavitation patterns

Hand drawn sketches of cavitation patterns may be used to describe cavitation in test reports. Schematic patterns are shown below in Figure 6 for various cavitation types.

Schematic pattern	Meaning
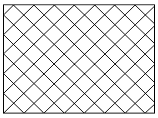	Stable sheet cavitation
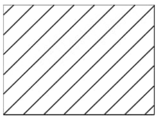	Temporarily unstable sheet cavitation
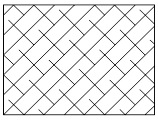	Unstable or fluctuating sheet cavitation
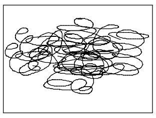	Cloud cavitation
	Streak cavitation
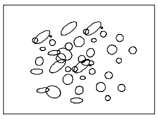	Bubble cavitation
	Thin stable tip/hub vortex cavitation
	Unstable tip/hub vortex cavitation
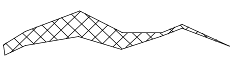	Thick stable tip /hub vortex cavitation
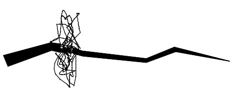	Bursting vortex cavitation

Figure 6: Schematic patterns for use in cavitation hand sketches

2.5 Non-stationary appearance of cavitation

A hand sketch (Figure 7) showing the extension of cavitation on the suction side (and, if required, on the pressure side) of a blade at different angular positions (every 20° in the case illustrated), with the radii of 0.5-0.6-0.7-0.8-0.9-0.95 marked on the blade, is often used to describe the changes of cavitation at the operating conditions of the propeller.

Adequate reporting of model cavitation patterns should include some or all of the following:

A) Display of still photographs or sketches of suction side and pressure side cavitation.
B) Notes as to the character of the fluctuations and unsteadiness associated with the above patterns. When using still photography, at least three photographs of each condition are recommended to document the level of cavity fluctuation.
C) Video presentation of both suction side and pressure side cavitation on the blades. If available, high-speed recordings are recommended to document the cavitation dynamics.
D) Display of any special cavitation regions on the propeller such as at the blade root and hub.
E) Discussion and interpretation of each cavitation type encountered and range of accuracy.

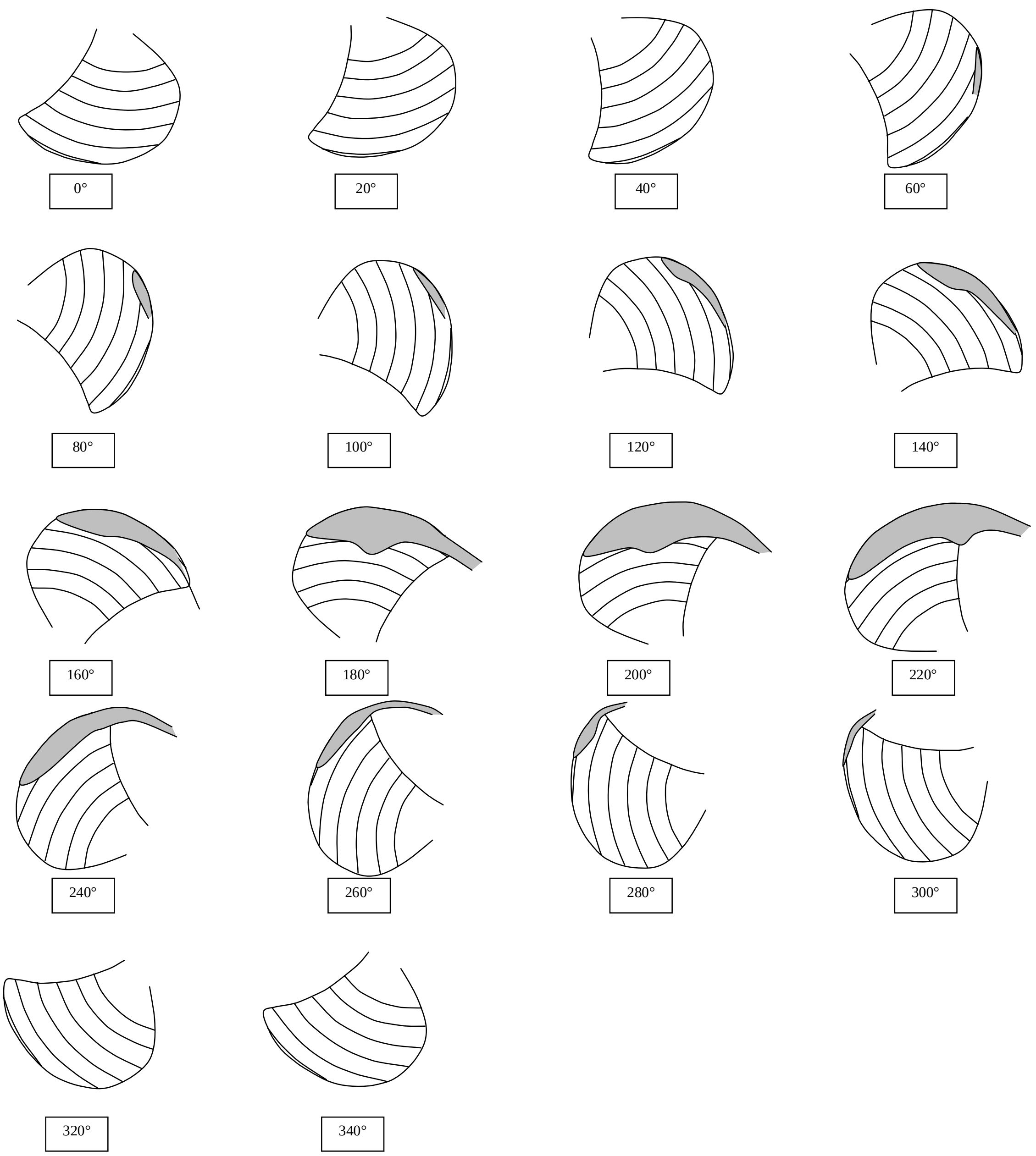

Figure 7:Suction side cavitation as a function of blade angular position

3. VISUAL DESCRIPTION OF CAVITATION ON PODDED PROPULSORS

3.1 Introduction

Descriptive terms are used to identify the various types of cavitation observed during tests on podded propulsors, typified below in Figure 8.

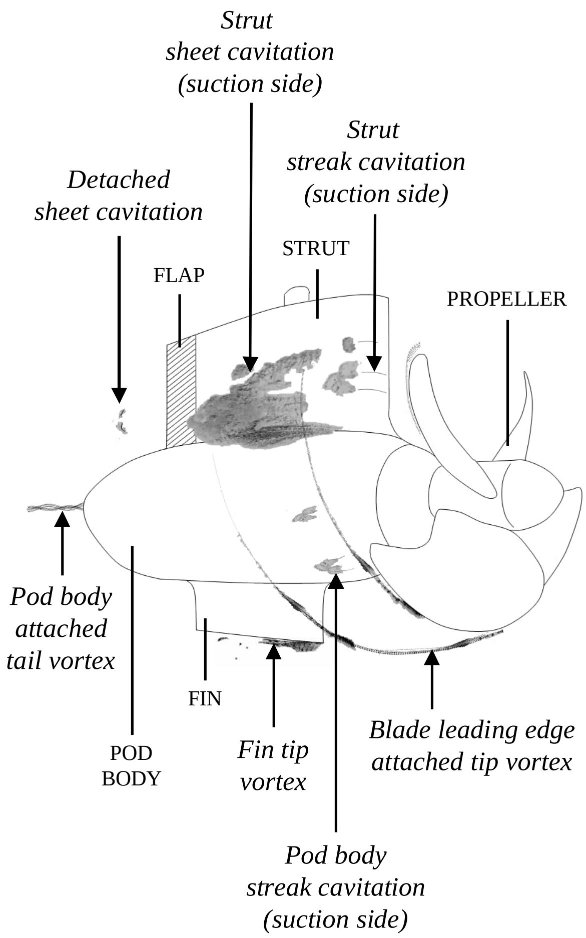

Figure 8: A representative pulling-type podded propulsor at a high azimuth angle and the associated cavitation types

Description of cavitation events should contain information on cavity location, size, structure, and dynamics, as well as proper references to the prevailing flow dynamics. The number of alternative descriptions for cavity structure should be limited to the most commonly used.

3.2 Description

The following descriptive types of cavitation on each component of a typical podded propulsor (i.e. propeller, pod body, strut, flap and fin) are recommended:

- vortex – attached and detached trailing; leading edge; hub (on pushing type); pod body tail (on pulling type)
- sheet
- bubble type – large, small
- streak
- cloud
- root
- supercavitation.

Along with the categories mentioned above, information on cavity location should be specified. The same specification used for conventional propeller can be used and extended for cavitation on the podded propulsor as follows:

- **Propeller**
  - radial location
    - fraction of tip radius
    - blade tip
    - root/fillet
    - tip (duct) gap
    - hub
  - chordwise location
    - fraction of chord
    - leading edge
    - trailing edge
  - suction side
  - pressure side
  - location in wake.

- **Pod body, strut, flap, fin**
  - chordwise and spanwise location
    - fraction of chord and span

  - leading edge and/or trailing edge
  - top and/or bottom end
- suction side
- pressure side
- location in wake.

Cavity size should be determined in terms of appropriate body dimensions of the respective component of the propulsor, if developed cavitation exists, e.g. by defining the fraction of the area of propeller blade, fraction of the projected area of the strut/pod body/flap/fin etc, which is covered by a given type of cavitation.

Typical cavity types that are observed on a high-speed, pulling-type podded propulsor model in a cavitation tunnel, are shown in Figure 9 and Figure 10.

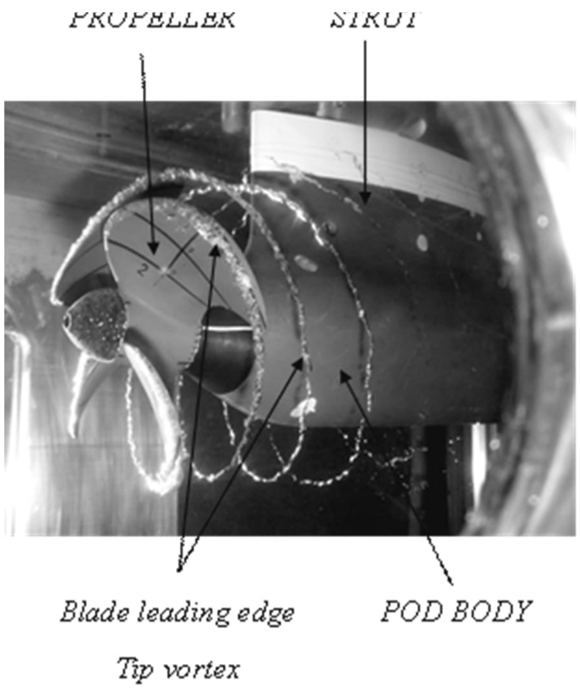

Figure 9: Attached blade leading edge tip vortex cavitation observed on a podded propulsor model set at 0° azimuth angle

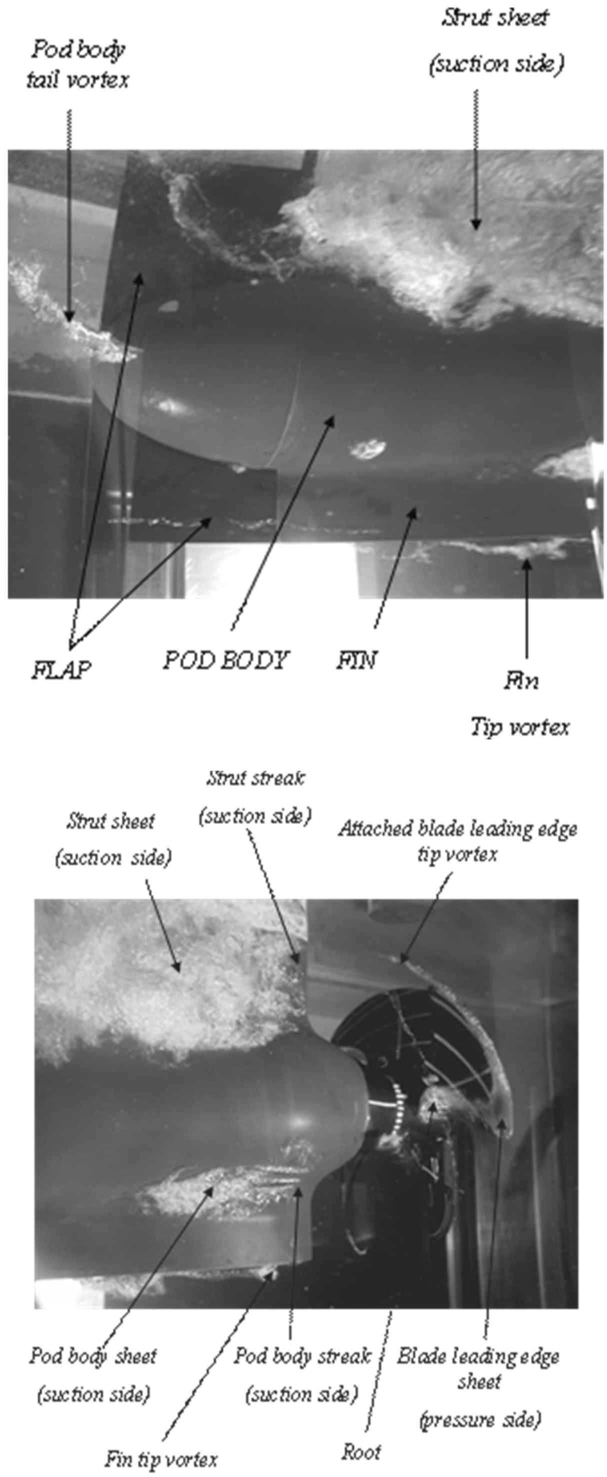

Figure 10: Cavitation types observed at the aft part (top) and fore part (bottom) of a high-speed podded propulsor model at 10° azimuth angle

Description of prominent types of cavitation (i.e. vortex, sheet, cloud, bubble etc), categorization of cavity dynamics (i.e. steady, unsteady, periodic etc) and flow regime associated with certain cavitation phenomena (i.e. laminar/turbulent boundary layer, steady/unsteady flow, separated, ventilated etc) should be stated. The description should be as complete as possible.

3.3 Propulsor model marking

Similarly to the marking of a conventional propeller, see Section 2.3, location and extent of the cavitation developing on other components of the podded propulsor can be established with a suitable grid (with adequate density) marked on the port and starboard sides of the pod housing. A sample grid system based on "maximum strut length" is shown in Figure 11.

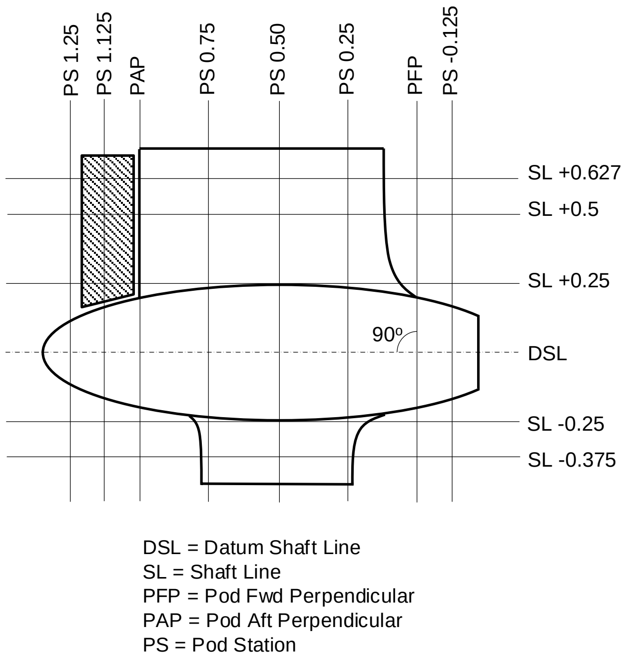

Figure 11: Sample grid definition to describe location and extent of cavitation on pod housing (to be applied on both sides of the housing)

3.4 Reporting cavitation patterns

Hand drawn sketches and other visual descriptions of cavitation patterns on the propeller are described in Sections 2.4 and 2.5. For a podded propulsor, reporting should be extended to include some or all of the following:

A) Display of still photographs or sketches of suction side and pressure side cavitation for all the relevant blade positions at specified azimuth and/or flap angles, if the latter two are required.
B) Display of still photographs or sketches of cavitation observed on other components of the propulsor (i.e. strut, pod body, fin, flap etc) at specified azimuth and/or flap angles, if the latter two are required, and on both the pressure and suction sides of the pod.
C) Notes as to the character of the fluctuations and unsteadiness associated with the above patterns. When using still photography, at least three photographs are recommended for each condition to document the level of cavity fluctuation.
D) Video presentation of both suction side and pressure side cavitation on the blades and cavitation on other components of the propulsor unit, relating them to each other (e.g. trajectories of blade tip vortex striking the strut, fin, etc, in pulling type). If available, high-speed recordings are recommended to document the cavitation dynamics.
E) Display of any special cavitation regions on the propeller such as at the blade roots, hub (in pushing type) and on other parts of the propulsor, such as pod body tail vortex, fin tip vortex, etc, and their possible interactions.
F) Discussion and interpretation of each cavitation type encountered and range of accuracy.

4. MEASUREMENT OF CAVITATION EVENTS

4.1 Introduction

Photographs or high-speed video recordings of cavitation patterns can be analysed to provide quantitative information about cavity location, size, structure, and dynamics. The information can be combined with and correlated to other measured quantities, such as pressure, noise, forces on blades, thrust and torque, velocity field. See sections 2 of 7.5-02-03-03.1, 7.5-02-03-03.3 and 7.5-02-03-03.9, and Guideline on Best Practices for the Applications of PIV/SPIV in Towing Tanks and Cavitation Tunnels (7.5-02-01-04).

4.2 Measurement of cavitation events

Cavitation extension over a propeller blade can be extracted from a single photograph, provided a reference photograph is taken in non-cavitating conditions, and a mapping calibration matrix is applied, see Figure 12 (Pereira et al, 2004).

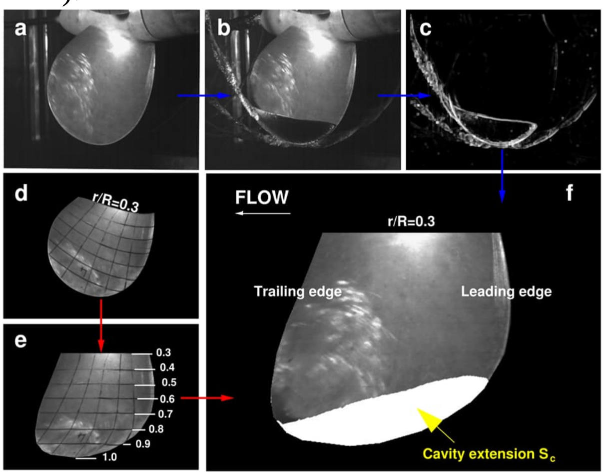

Figure 12: (a) no-cavitation image; (b) cavitation image; (c) correlation image; Mapping procedure: (d) distorted image; (e) plan-view image; (f) processed image showing the cavitation extension

Thickness and volume of an attached leading-edge cavity can be measured using non-intrusive techniques: photogrammetry techniques (Lehman, 1966; Ukon and Kurobe, 1981; Savio et al, 2009; Shiraishi et al, 2017), laser line projection and ultrasound pulsed echography (Felici et al, 2013). Volume of cloud cavitation can be measured using tomographic reconstruction (Pereira et al, 1998). In the lack of such measurements, a cavity equivalent volume can be approximated from the cavity extension measurement based on a characteristic length, such as the square root of the cavity area. The same approach can possibly be extended to other forms of cavitation.

4.3 Measurement of unsteady cavitation events

High-speed visualizations provide time-resolved information about the cavitation state during the propeller revolution, see Figure 13. This approach is recommended for unsteady cavitation events, as in a periodically varying pressure field (e.g. skeg wake, rudder, pod, other appendages).

Cavitation extension, and equivalent volume derived from cavitation extension, can be quantified applying the procedure described in Section 4.2 (Alves Pereira et al 2016).

4.4 Cavitation viewing and lighting

Visualization can be done through viewing ports in the tunnel walls, unless the test section is equipped with large transparent windows. When testing a propeller behind a hull, such as in a large cavitation tunnel or a depressurized towing tank, video or high-speed cameras can be installed in watertight, pressurized housings positioned beside the hull, or through ports in the hull located close to or over the propulsor. In this latter case, boroscope-based systems are an alternative solution, although imaging may suffer from noticeable optical distortions and aberrations.

The recommended set-up for the viewing axis is (close to) normal to the cavitating surface, e.g. the blade, to minimize optical out-of-focus, maximize field-of-view and improve measurement accuracy. However, this often implies tilting the photographic apparatus or digital camera at an angle with respect to the viewing port or window. This introduces strong optical aberrations, which are typically taken care of by placing a water prism in between the camera lens and the viewing interface, thus repositioning the optical axis in a perpendicular orientation. This solution is difficult to implement on board of a ship model, in which case a boroscope-based approach is recommended.

For standard visualization, adequate lighting is required to image the pattern at specific angular positions throughout the cavitating region of the disk. For real time visual observation, single-flash lighting is preferred, synchronized on the propeller rotation pulse along with adequate phase delays. Alternatively, continuous, high-power light sources can be used for time-resolved visualizations with high-speed cameras, see Section 4.3. Daylight sources, such as HMI- or LED-type, are recommended to avoid overheating of the viewing ports or windows, and instrumentation in the vicinity.

In general, a lighting set-up needs a case-to-case adjustment depending on many parameters such as the laboratory environment, the illumination power available, the light sensitivity (or collection efficiency) of the imaging instrumentation, and the type of cavitation. For instance, back lighting should be used to illuminate cavitation inception, which is very difficult to detect with front lighting.

The viewing arrangement should be duplicated if both back and face cavitation need to be recorded and described simultaneously. The two visualization subsystems should be duly synchronized.

4.5 Time-lapse video

Standard video in general is not a sufficient tool to analyse the dynamics and structures of the different cavities; nevertheless, it is a useful supplement. One should consider the following points:

- The pixel resolution of standard video is usually higher compared to high-speed video.
- It is easier to switch between different sources of light during the recording thus giving more information on the cavitation process.
- Standard video is superior when concerned with the recording of intermittency and long-term fluctuations of the cavitation process. This is very important as a supplement to the paint tests.
- Overview videos can be added as a supplement to high-speed videos to analyse the development of focusing cavities from the global cavity.
- Exposure and lighting can be varied to show different details, thus allowing an inspection of the cavities in real time during recording. Camera shutter time should be tuned to minimize motion blur without compromising image quality.

4.6 High Speed video

The true development and dynamics of a specific cavity can only be seen by recordings of a high-speed film or, preferably, digital high speed video technique. For commercial use, the high-speed video technique is recommended. The following guidelines should be considered:

- The frame rate, exposure time of an individual frame and the duration of the total recording are the primary parameters that have to be considered. The exposure time is partly related to the frame rate. The requirements on these parameters are related to the water velocity and propeller rate of revolution.
- In a typical propeller experiment with an advance velocity of up to approximately 10 m/s, exposure times from 1/10000 s or shorter are usually sufficient to avoid motion blur. A lower limit for the frame rate may be around 3000 frames/s but a value between 4000 and 7000 is significantly more useful. Frame rates as low as 1000 frames/s are found to be inadequate for analysis.
- As for standard video, small lens apertures are required for sufficient reduction of optical aberrations, which degrade the sharpness, and for obtaining a sufficient depth of field (or depth of focus). The most effective way to control aberrations and depth of field is to select an optimal camera position and to have enough light. Optical elements like prisms and correction lenses can also be helpful.

In practice, when filming objects moving in space, the resolution is influenced by the following parameters:

- scale of reproduction (field of view)
- motion of the object (revolution rate)
- exposure time (shutter speed)
- extent of the object along the optical axis (depth of field)
- lens aperture (depth of field)
- sensor resolution (pixels per mm)
- contrast of the object
- frame rate (revolution rate).

Some of the listed parameters are interrelated, in theory as in practice. Most of the parameters can be modified by the operator and need to be optimized according to the specific test set-up.

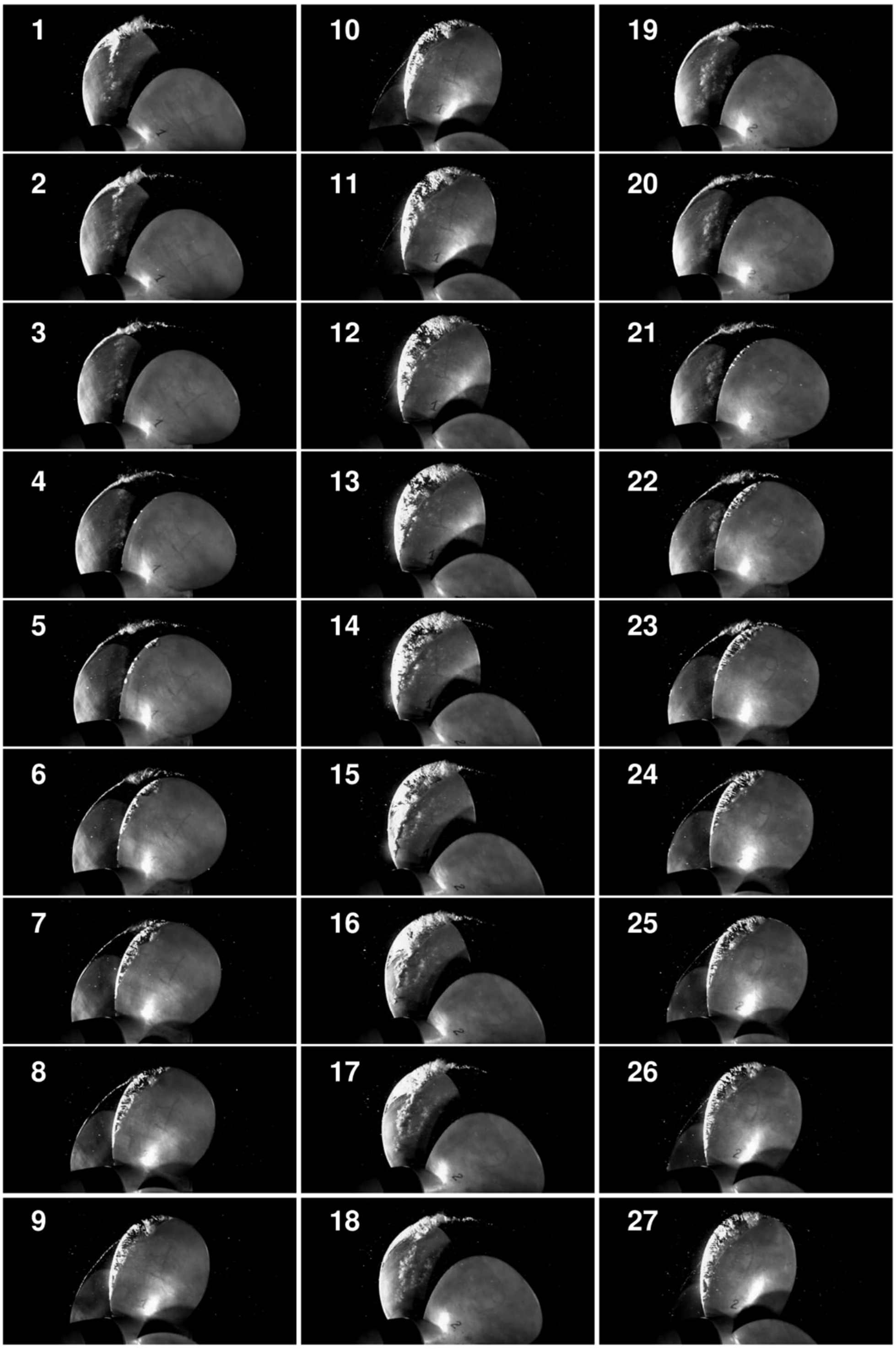

Figure 13: High-speed sequence of unsteady leading edge cavitation on propeller blade. Inter-frame time = 500 µs, angular step = 5.4◦ . Flow is from left to right; view of the propeller suction face, port side.

4.7 Uncertainty and output datasets

For the purpose of CFD validation (see for instance procedure 7.5-02-03-03.4 “Cavitation-Induced Pressure Fluctuations: Numerical Prediction Methods”), all measurements should provide an indication of the uncertainty of the experimental methodology. Quantities should be provided in terms of mean values and of fluctuations (e.g. standard deviation or root-mean-square).

Results from cavitation measurements should be represented in terms of cavitation extension over the blade in a CFD-equivalent reference system for accurate comparison, e.g. plan-view as in Figure 12(f). Quantities to be provided are: cavitation mean area as fraction of a reference blade area (e.g. expanded area of a propeller blade); standard deviation of cavitation area; equivalent volume (mean and standard deviation). Mean and standard deviation can be relative to one specific blade. To account for blade-to-blade variations of the cavitation pattern due to blade manufacturing uncertainties, or pitch setting uncertainties, statistics can be made over several blades and supported by high-speed video recordings. Original photographs or images should be made available for reporting and comparison with computations.

Each measurement should be accompanied with the relevant operating test parameters (mean values, and standard deviation if available): static pressure, rotation rate, upstream flow velocity, cavitation number, advance ratio. Additional data to be included: thrust, torque, noise, wall pressure data, etc.

5. CAVITATION INCEPTION

5.1 Test performance

Cavitation inception tests consist of plotting observed cavitation points in a diagram of cavitation number (σn) versus advance ratio (J). Points for the same type of cavitation are connected to determine inception boundaries of each form of cavitation. At least three inception points should be determined to describe an inception curve. More inception points will reduce the uncertainty in defining the inception curve. A sample diagram of this type is displayed in Figure 14.

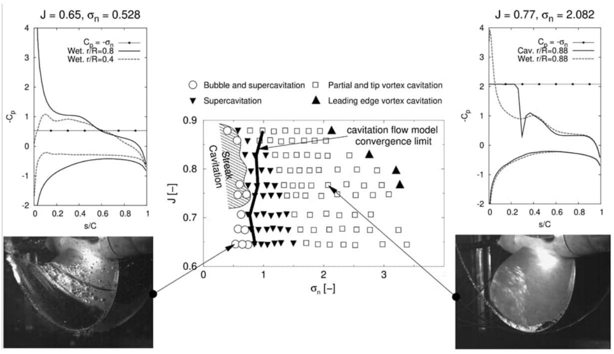

Figure 14: Cavitation types as a function of cavitation number and advance ratio

The tip vortex cavitation inception for model propellers should be scaled with the Reynolds number. Scaling of other forms of cavitation is not considered routine and would require justification supported by credible data.

Cavitation inception tests should be performed by experienced personnel in a consistent fashion. Inception is observed when an event is seen at a given interval, such as 1 or 10 seconds between events. Care must be taken if the interval between events is too long to distinguish real from random events. For cavitation inception on blades, tests can be made on a number of blades, i.e. a majority of blades, or on one blade. One-blade tests are not recommended due to possible effects of geometric flaws. Determining the point of disappearance, or desinence, of cavitation can be an acceptable alternative to inception determination. Inception or desinence criteria should be stated in the cavitation report.

For a podded propulsor, detection of cavitation inception can also be performed on the prominent locations of the other components of the system, e.g. strut leading edge, fore and tail end of pod body, flap and fin tips, etc.

5.2 Acoustic cavitation inception

Cavitation inception can occur before visual observation, and acoustic measurements often give a cavitation number higher than the one obtained through visual inspection. Using a hydrophone, one can determine acoustic cavitation inception - or sub-visual cavitation inception - by measuring the sound pressure level (SPL) produced by the device under test conditions of constant velocity and at a series of tunnel pressures. Acoustic cavitation inception occurs when the level and/or frequency content of the measured SPL increases. The advantages of acoustic cavitation detection are the quantitative nature, the consistency, and the earlier detection over visual methods. The disadvantages include the difficulty of setting up the test, the inability to discriminate extraneous cavitation noise sources, and the potential masking by other noise sources. Furthermore, acoustic cavitation detection does not allow for the classification of the type of cavitation.

Acoustic detection of cavitation inception, used in combination with or as alternative to visual detection, should be used with care since no discrimination between cavitation types is guaranteed. Furthermore, acoustic inception can be used only to detect the first form of cavitation appearance. Moreover, one must be aware that the first form of cavitation occurring at model scale may not be the same at full scale.

5.3 Water quality

An important part of the inception test set-up phase is to know the water quality of the test facility. This includes some knowledge of the nuclei size distribution, liquid tension as well as dissolved gas content[1]. Nuclei distributions and liquid tension data can be correlated to online gas content measurement in most facilities to estimate water quality during cavitation testing. Systematic procedures must be implemented to consistently achieve a reference water quality before testing. Cavitation inception curves should be correlated for water quality effects, as discussed in the report of the 23rd ITTC Specialist Committee on Water Quality and Cavitation (2002).

The influence of water quality, quantified indirectly by the dissolved gas level or directly as a microbubble/nuclei population measurement, is known to impact the inception and development of cavitation, and therefore its scaling and the associated flow/hull pressure fluctuations and propagation of noise into the surrounding environment. Water with too few nuclei may delay cavitation inception as it is known from conventional cavitation testing. On the other hand, too high gas content can lead to gaseous cavitation, or pseudo-cavitation instead of the vaporous cavitation. This may introduce a damping/cushioning effect to the cavitation collapse and will reduce its effects and provide unreliable results. Such a condition may also deteriorate the visibility inside the tunnel and make the observation, e.g. of focusing cavities, rather difficult or even impossible. It is also generally accepted that testing at relatively high gas content

[1] Also intended as air content or oxygen content depending on each facility's testing capabilities and procedures.

modifies the population of nuclei in a water tunnel facility, reduces the tensile strength and improves the correlation of noise between model and full-scale data.

The relation between gas content α or gas content ratio αs and nuclei is dependent on the facility (23rd ITTC Specialist Committee on Water Quality and Cavitation, 2002). Nuclei populations can differ between facilities for comparable dissolved gas levels and vary in time within a particular facility. Whereas the dissolved gas content, and specifically the dissolved oxygen content, can easily be measured, the measurement of the nuclei concentration is much more complicated. Some water tunnels have been designed to control the nuclei population independently of the dissolved gas level but in general this is not the case. The Final Report of the 29th Specialist Committee on Hydrodynamic Noise (2021) provides a review on the techniques available for nuclei size and population measurements.

Hence, the optimum gas content for a given cavitation facility should be determined by long-established experience. To enhance the consistency of the measurement results, it is recommended that the tensile strength of the water in the facility be checked periodically. In the case of water tunnels where the nuclei content is controlled by measuring the gas content, the gas content is typically between 30% and 70% of the saturation rate at atmospheric pressure. In water tunnels where the nuclei content is controlled independently of the gas content, this latter is in the order of 30% of the saturation rate at atmospheric pressure. In a towing tank, electrolysis can be applied to supply nuclei, and the gas content is about 30% of the saturation rate at atmospheric pressure.

When there are insufficient concentrations of nuclei, all forms of cavitation behave intermittently at model-scale. Cavitation on the model propeller blade is sometimes stabilized through controlled roughness by layering sand grain in the vicinity of the leading edge, or through electrolysis in the boundary layer flow along the hull (26th Specialist Committee on Cavitation Induced Erosion on Propellers, Rudders and Appendages - Model Scale Experiments). The sand grain size should be carefully chosen in relation to Reynolds number to minimize the effect on cavitation inception number (21st Report of the ITTC Propulsor Committee, 1996).

6. PARAMETERS

See sections 2.11, 3.1 and 3.2 of 7.5-02-03-03.1.

6.1 Basic measurement quantities

D	propeller diameter	(m)
R	propeller radius	(m)
p_A	ambient pressure (representative static pressure at the point of interest)	(Pa)
n	propeller frequency of revolution	(Hz)
V_T	tunnel velocity	(m/s)
V	ship speed	(m/s)
T	thrust	(N)
Q	torque	(N.m)
t_W	water temperature	(°C)
r	blade section radius	(m)
α	gas content	(ppm)
α_S	gas content ratio	(%)
ω	propeller rotational velocity	(rad/s)

6.2 Derived parameters

V	ship speed	(m/s)
V_A	propeller advance speed	(m/s)
V_T	resultant velocity	(m/s)

$$V_T=(V_A^2+\omega^2 r^2)^{1/2}$$

V_0	representative speed: V, V_A, V_T, nD or ω_r	(m/s)
J	propeller advance ratio	(-)

$$J=V_A/(nD)$$

σ_V vapour cavitation number (-)

$$\sigma_V = (p_A - p_v) / (0.5\rho V_0^2)$$

σ_n propeller cavitation number (-)

$$\sigma_n = (p_A - p_v) / (0.5\rho n^2 D^2)$$

K_T thrust coefficient (-)

$$K_T = T / (\rho n^2 D^4)$$

K_Q torque coefficient (-)

$$K_Q = Q / (\rho n^2 D^5)$$

p_V vapour pressure of water (Pa)

5 BENCHMARK TESTS

1. Comparative Propeller Tests (7th 1955 pp.129-216) The Completion of the Full Programme of Tests in One Tunnel

   a) Tests of at least one model propeller in each of the eight tunnels
   b) Completion of the open-water tests of all the model propellers in ship tanks
   c) Measurement of all the model propellers, including surface finish propeller models from 8 to 18 inches diameter at Reynolds' number from 1.5 to 7.5 million

2. Cavitation Tunnel Tests of Series 1 Propellers (7th 1955 pp.131-135) Parent Model AEW/C2 (Diameter 9-12-15-18)

3. Cavitation Tunnel Tests of Series 2 Propellers (7th 1955 pp.135-168)
   3-Bladed Propeller; Developed Blade Area Ratio 0.655; Pitch Diameter Ratio 1.33; Constant Ogival Sections with Sharp Leading Edges; Design Advance Coefficient J=0.925

4. Cavitation Tunnel Tests of Series I 12 Inch Propellers and Series III 12 inch Propellers (7th 1955 pp.169 - 189)
   Series I: 12 Inch Propeller in All Tunnels
   Series III: 12 Inch Propeller in Tunnels
   Tunnel Wall Effect: less than 0.14

5. Open Water Tests of Model Propellers (7th 1955 pp.190 -199)
   Series I: Tested in No.2 Ship Tank Haslar
   Series II: Tested at Carderock
   Series III: Tested at Gothenburg

6. Tolerance and Surface Finish of Model Propellers (7th 1955 pp.200-216)

7. Cavitation Inception on Head Forms Comparative Experiments (11th 1966 pp.170)

8. Cavitation Inception on Head Forms ITTC Comparative Experiments (11th 1966 pp.219-232)

   a) Cavitation number for cavitation inception on the body

   b) Cavitation number when bubbles are clearly visible in the test section in front of the body i.e. when the resorption power of the tunnel is no longer sufficient.

9. 1TTC. Standard Screw Cavitation Tunnel Tests at Brodarski Institute (12th 1969 pp. 523-525) 228.6 mm Diameter

10. Nuclei Measurement and "Standard Cavitator" (13th 1972 pp.642-646)

    a) Air Content- and Nuclei Measurement

    b) "Standard Cavitator"

11. Comparative Hydrofoil Experiments and Development of a Standard Cavitator (14th 1975 Vol.2 pp.76-93)

    a) Results of Tests with Three-Dimensional 19-012 and 16-1512 Hydrofoils in Different Cavitation Facilities

b) Progress in the Development of a 'STANDARD CAVITATOR’

12. Appendix A (Hydrofoils) (15th 1978 pp.340-347)

a) Foil F: Symmetrical Profiles NACA 19-012

b) Foil G: Cambered Profiles NACA 19-1512

13. Comparative Tests with the Foil-Head form Combination (16th l981 pp.420-424)

14. Comparative Noise Measurements with the Sydney Express Propeller Model (16th 1981 pp.447-453)

15. Comparative Tests on Soft Surface Techniques (16th 1981 pp.436-443)
The SSPA Stencil Ink Method, Modified by SRI-MHI Test Procedure

16. Comparative Tests with Foil-Headform Combination (17th 1984 pp.245-248)

17. Comparison of Hull Pressure Amplitudes for Sydney Express Propeller (17th 1984 pp.248-252)

18. Comparative Erosion Tests with Propeller Model (17th 1984 pp. 252-255)

19. Comparative Noise Measurement with Sydney Express Propeller Model (17th 1984 pp.255-256)

20. Comparative Cavitation Observations on Propeller with and without Leading Edge Roughness (18th 1987 pp.207 -208) Model Propeller; NSMB Model 6091, as the '18th ITTC Propeller'

21. Comparison of Propeller-Induced Hull Pressure Measurements for the "SYDNEY EXPRESS" Propeller Models (18th 1987 pp.209-210)

22. Comparative Noise Measurements with "SYDNEY EXPRESS" Propeller Models (18th 1987 pp.210~-211)

23. Cavitation Nuclei Measurements (19th 1990 pp.166-175)

24. Propeller-Induced Hull (19th 1990 pp.182-187)

25. Further Measurement of Pressure Fluctuation on 'SYDNEY EXPRESS' Propeller (19th 1990 pp.213-219)

26. Joint Bassin d’Essais des Carènes and Cavitation Committee Tests (20th 1993 pp.206-213)
Measurement of Liquid/Nuclei Distribution Determination of Cavitation Inception Scale Effects. Minimizing the Liquid Tension in a Water Tunnel or Towing Tank.

27. 20th ITTC Comparative Model Measurements (20th 1993 pp.230-231)
Measurements on German Tanker "St. Michaelis" and the "Sydney Express"

28. Comparative Measurement of Pressure Fluctuation on the "St Michaelis" (20th 1993 pp.236-240)

29. Measurements of Hull Pressure Fluctuation (21st 1996 pp.65-69

7. REFERENCES

Alves Pereira F, Di Felice F and Salvatore F (2016). Propeller Cavitation in Non-Uniform Flow and Correlation with the Near Pressure Field. Journal of Marine Science and Engineering, 4, 70, DOI:10.3390/jmse4040070.

Felici A, Di Felice F and Alves Pereira F (2013). Measurement of the Cavitation Pattern by Two Non-Intrusive Techniques: Laser Imaging and Ultrasound Pulsed Echography. Exp. Fluids, 54:1482, DOI: 10.1007/s00348-013-1482-x.

Lehman A F (1966). Determination of Cavity Volumes Forming on a Rotating Blade. 11th International Towing Tank Conference (ITTC), Tokyo (Japan), pp. 250–253.

Pereira F, Avellan F and Dupont P (1998). Prediction of Cavitation Erosion: An Energy Approach. J Fluid Eng - T ASME, 120(4):719–727.DOI: 10.1115/1.2820729.

Pereira F, Salvatore F and Di Felice F (2004). Measurement and Modelling of Propeller Cavitation in Uniform Inflow. J Fluid Eng – T ASME, 126:671–679. DOI: 10.1115/1.1778716.

Savio L, Conti F, Viviani M, Ferrando M (2009). Application of computer vision techniques to measure cavitation bubble volume and cavitating tip vortex diameter. Proceedings of the 7th International Symposium on Cavitation (CAV2009), August 17-22, 2009, Ann Arbor, Michigan, USA.

Shiraishi, K., Sawada, Y. and Hoshino, K., “Cavity Shape Measurement Using Combination-Line CCD Camera Measurement Method”, Proc. of the Fifth International Symposium on Marine Propulsion SMP’17, Espoo, Finland, June 2017, n° 1214.

Ukon Y and Kurobe Y (1981). Measurement of Cavity Thickness Distribution on Marine Propellers by Laser Scattering Technique. Proc. of the 16th ITTC, vol. 2, , Leningrad (USSR), pp. 241–245.

8. KEYWORDS

ITTC; guideline; procedure; cavitation; visualization; description; measurement; inception; model scale